ANNALS of Clinical and Translational Neurology
Open Access
ANA American Neurological Association since 1875

RESEARCH ARTICLE

Impact of Zika Virus on adult human brain structure and functional organization

Richard Bido-Medina[1,2], Jonathan Wirsich[1], Minelly Rodríguez[3], Jairo Oviedo[4], Isidro Miches[2], Pamela Bido[3], Luis Tusen[3], Peter Stoeter[4] & Sepideh Sadaghiani[1,5]

[1]Beckman Institute for Advanced Science and Technology, University of Illinois at Urbana-Champaign, Urbana, Illinois 61801
[2]Neuroscience Program, University of Illinois at Urbana-Champaign, Urbana, Illinois 61801
[3]Hospital Salvador B. Gautier, Santo Domingo, Dominican Republic
[4]Centro Diagnostico de Medicina Avanzada y Telemedicina (CEDIMAT), Santo Domingo, Dominican Republic
[5]Psychology Department, University of Illinois at Urbana-Champaign, Urbana, Illinois 61801

Correspondence
Richard Bido-Medina, University of Illinois at Urbana-Champaign, Beckman Institute for Advanced Science and Technology, 405 N Mathews Ave, Urbana, IL-61801. Tel: 217-300-2566; Fax: 217-300-2922; E-mail: bidomed2@illinois.edu

Funding Information
No funding information provided.

Received: 16 March 2018; Revised: 12 April 2018; Accepted: 13 April 2018

Annals of Clinical and Translational Neurology **2018; 5(6): 752–762**

doi: 10.1002/acn3.575

Abstract

Objective: To determine the impact of Zika virus (ZIKV) infection on brain structure and functional organization of severely affected adult patients with neurological complications that extend beyond Guillain–Barré Syndrome (GBS)-like manifestations and include symptoms of the central nervous system (CNS). **Methods**: In this first case–control neuroimaging study, we obtained structural and functional magnetic resonance images in nine rare adult patients in the subacute phase, and healthy age- and sex-matched controls. ZIKV patients showed atypical descending and rapidly progressing peripheral nervous system (PNS) manifestations, and importantly, additional CNS presentations such as perceptual deficits. Voxel-based morphometry was utilized to evaluate gray matter volume, and resting state functional connectivity and Network Based Statistics were applied to assess the functional organization of the brain. **Results**: Gray matter volume was decreased bilaterally in motor areas (supplementary motor cortex, specifically Frontal Eye Fields) and beyond (left inferior frontal sulcus). Additionally, gray matter volume increased in right middle frontal gyrus. Functional connectivity increased in a widespread network within and across temporal lobes. **Interpretation**: We provide preliminary evidence for a link between ZIKV neurological complications and changes in adult human brain structure and functional organization, comprising both motor-related regions potentially secondary to prolonged PNS weakness, and nonsomatomotor regions indicative of PNS-independent alternations. The latter included the temporal lobes, particularly vulnerable in a range of neurological conditions. While future studies into the ZIKV-related neuroinflammatory mechanisms in adults are urgently needed, this study indicates that ZIKV infection can lead to an impact on the brain.

Introduction

Since the beginning of the current Zika virus (ZIKV) outbreak in 2015, 3–4 million adults have been infected, a subset of which has suffered severe neurological complications.[1] According to the WHO, 79 countries have reported ZIKV systemic infections as of March of 2017, including 21 with documented neurological syndromes in adults.[2] ZIKV has been known since 1947 and several studies have pointed to the virus' neurotropism and its potential to cause neural damage.[3] Surprisingly, the causal association of the virus with clinically relevant neurological manifestations is recent. In consonance with the increased rate of microcephaly associated with ZIKV in pregnant women,[4] the majority of efforts have been devoted to understanding such unfortunate developmental disruptions. ZIKV-related neurological complications in adults have been overlooked, and the understanding of such a nosological entity remains significantly limited.

Evidence supporting the association of ZIKV infections with neurological complications in adults is increasing.[5] Most of the reported neurological complications consist of Guillain-Barré Syndrome (GBS), with incremented incidence during ZIKV outbreaks.[6–8] Remarkably, manifestations in ZIKV patients often deviate from traditional GBS, with rapid onset and progression,[6,9] nontypical descending pattern,[10] and CNS symptoms.[11,12] The documented number of cases affecting the CNS is growing, including entities like encephalitis, meningitis, meningoencephalitis and myelitis.[12–16] There are documented cases of patients reporting memory impairments, cognitive declines,[17] coma, positive Babinski sign, delusions and hallucinations.[18] Furthermore, the presence of the virus in the CNS has been demonstrated in the cerebrospinal fluid (CSF) in adult patients with CNS manifestations.[15,18] In summary, the growing evidence of ZIKV infection linked to neurological presentations ranges from peripheral nervous system (PNS)-exclusive alterations,[7,8] reported mixed PNS/CNS symptoms[11,15,18] to fatal CNS inflammatory disease.[16] Collectively, these observations suggest that neurological complications in ZIKV may extend beyond the PNS.

Consequently, there is an urgent need for case–control studies to neurobiologically characterize the relationship between ZIKV and CNS manifestations.[11] The current study focused on adult patients presenting ZIKV-related central neurological manifestations in addition to peripheral symptoms. Our main goal was to reveal and characterize potential structural and functional changes in the brain of adults with ZIKV-related neurological complications. The central hypothesis was that ZIKV patients whose neurological complications included central nervous manifestations would show changes in brain structure and functional organization. For this purpose, we acquired neuroimaging data in nine rare patients in the subacute stage of their neurological syndrome who presented with a variety of nonclassical GBS as well as CNS-exclusive symptoms (e.g., prosopagnosia, dysmorphopsia, and photophobia), and in matched healthy controls. Data were acquired in the Dominican Republic, endemic for Aedes mosquito-borne diseases. We focused analysis efforts on gray matter volume and resting-state functional connectivity (rsFC). Gray matter volume morphometry has proven informative in other PNS diseases with axonal damage[19,20] and central inflammatory processes (both infections[21–23] and noninfectious[24,25]). Regarding brain function, whole-brain network analysis of rsFC has proven a powerful tool to elucidate distributed functional brain reorganization due to neuroinflammation, and to contribute clinically useful key prognostic indicators,[26–28] for example, in virus-borne neuro-inflammations including *N*-methyl-D-aspartate receptor encephalitis and HSE.[29–31]

Materials and Methods

Participants

We acquired clinical and MRI data in nine patients (3 females, Age = 35 ± 4.46, range: 30–45 years) in the subacute stage (5 ± 0.5 months since onset of neurological symptoms) with at least one CNS-related manifestation as detailed in Table 1. Nine healthy age- and sex-matched controls also underwent MRI (see Table 1). Recruitment and clinical assessment occurred at Hospital Salvador B. Gautier, Santo Domingo, Dominican Republic, and MRI data were acquired at Centro de Diagnóstico Medicina Avanzada y Telemedicina (CEDIMAT), Santo Domingo, Dominican Republic. All subjects gave written informed consent according to procedures approved by the Internal Review Boards of the University of Illinois at Urbana-Champaign, IL, USA, Hospital Gautier, and CEDIMAT. All patients presented an abrupt onset of neurological deterioration with variable time periods between systemic manifestation and neurological symptoms. Only patients with stable cognitive and clinical status were MRI-scanned (Mini Mental State Examination ≥ 23 and Glasgow scale ≥ 13).

Immunologic testing was used to confirm previous ZIKV infection (IgM/IgG enzyme-linked immunosorbent

Table 1. Demographic and clinical data of ZIKV patients included in the study.

	Patients (*N* = 9) M (±SD)	Controls (*N* = 9) M (±SD)
Gender (Female)	3	3
Age (range 30–45 years old)	35 (±4.46)	32 (±5.91)
Period between ZIKV onset and MRI scan (months)	5.6 (±1.5)	
Period between ZIKV onset and neurological manifestations (days)	8.8 (±4.91)	
Guillain–Barre variant (# of patients with descending pattern)	6	
Hughes scale at admission	3.2 (±0.97)	
Hughes scale at discharge	2.3 (±0.87)	
Atypical and CNS manifestations	Acute	Subacute (scan)
Loss of visual acuity	1	1
Diplopia	4	4
Intense headache	2	0
Photophobia	1	0
Eye pain	1	0
Facial Diplegia	6	5
Vertigo	1	1
Prosopagnosia	1	1
Hyperacusis	1	1
Dysmorphopsia	1	1

assay (ELISA) serum levels > 1.1 mg/dL), and to exclude Herpes Simplex 1 (HSV-1). Additionally, other possible causes for the febrile syndrome (Dengue, Chikungunya, Malaria, Leptospirosis, Mononucleosis infecciosa, and HIV primo-infection) were excluded using immunological testing as specified in the febrile syndromes protocol of the Dominican Republic. HIV status was assessed using ELISA, and was reported negative for all patients. To rule out spirochete-related diseases with impact on the CNS (e.g., syphilis, Lyme's), Venereal Disease Research Laboratory (VDRL) was performed and reported negative for all patients.

Patients were diagnosed with a GBS-like syndrome by clinical manifestations and electromyography (EMG) in all patients, and CSF testing (i.e., albuminocytologic dissociation; see Clinical profile section) in eight of the patients. Nerve velocity conduction using EMG (EMG/NVC) was assessed by investigator L.T. during the acute stage. The exclusion of other entities with potential direct impact on the CNS, such as viral encephalitis, acute disseminated encephalomyelitis (ADEM), and meningitis were ruled out by the treating neurologists based on clinical manifestations, CSF test results, and EMG (see Clinical profile below for a detailed description). Disability due to the peripheral neuropathy was measured by Hughes modified scale at admission and discharge (see Table 1). In accordance with the Dominican Protocol (2016) for the management of GBS, patients were treated with immunoglobulins (2 g/kg divided in 2–5 doses of antibodies unlikely to affect brain function) during the first 5 days of onset of neurological manifestations. Patients did not receive specific medication or treatment at time of scan.

Clinical profile

Beyond one or more CNS-related manifestations in each patient in both acute and subacute phases (Table 1), GBS presentation in six patients showed atypical features in the form of onset with descending paresthesias, facial diplegia, dysphagia and/or dyspnea. The onset of the neurological symptoms occurred in a short period of time (8.8 days ($\pm$4.91)) from the Zika infection, and were abruptly disabling. T2/FLAIR images, acquired during subacute stage, were normal as assessed by neuroradiologist P.S. From the 9 patients, 8 exhibited an albuminocytologic dissociation of CSF markers, defined as elevated protein (>45 mg/dL, and up to 1800 mg/dL in our patients) without increase in white blood cell count (<10 cell/per mm^3). Albuminocytologic dissociation is a characteristic feature of GBS, present in around 90% of the cases.[32,33] The low pleocytosis is also an exclusion parameter for other entities like viral encephalitis, ADEM, meningitis, Citomegalovirus poliradiculitis and sarcoidosis, in which white blood cell is expected to be elevated (>50 cells/per mm^3).[33] The Mini Mental Status Examination did not show severe cognitive dysfunction at the onset of the neurological symptoms or at time of MRI scan (mean = 28.5, $\pm$2.2, range = 23–30, only one subject below 27). In all patients, EMG/NVC values during the acute phase were compatible with an acute demyelinating inflammatory polineuroradiculopathy with a mixed component (myelin + axonal damage) that was predominantly axonal.[34] Specifically, the findings showed prolonged latency (Upper Limb: >4.2 msec for motor and >3.6 msec for sensory; Lower Limbs: >5 msec for motor and >3.6 for sensory), including prolongation of F wave for both upper and lower limbs (>32 and >50, respectively). EMG/NVC also showed reduced amplitudes (Upper Limbs: <5 mV; Lower Limbs: <3.5 mV) and prolongation of NVC (Upper Limbs: >50 m/sec; Lower Limbs: >40 m/sec).

MRI data acquisition and processing

MRI was acquired on a 3 Tesla Philips Achieva scanner at CEDIMAT facilities and included: T2/FLAIR, T1/MPRAGE (TR/TE = 3000/2.6 msec, 180 slices, voxel size 1 mm^3, flip angle 90°), and 6 min eyes-closed resting-state fMRI (T*2/EPI sequence, TR/TE = 2000/30 msec, flip angle = 80°, in-plane matrix size of 80 x 80, voxel size 2.38 x 2.4 x 3 mm^3, slice gap = 0, 34 axial slices aligned to AC-PC plane). Head movement derived from fMRI did not differ between groups (Framewise displacement FD: $P = 0.931$; and DVARS measures of motion outliers[35] $P = 0.258$, Wilcoxon rank-sum test). Additionally, we compared the number of fMRI volumes that pass the FD and DVARS threshold (both at 0.5). The number of suprathreshold volumes did not differ significantly between controls and patients (FD: $P = 0.83$ and DVARS: $P = 0.47$, Wilcoxon rank-sum).

Since nonparametric permutation tests provide a control for false positives without strong a priori assumptions about the data, they are more robust for small sample sizes than more commonly applied parametric statistics.[36,37] In the following, we describe permutation-based statistics applied to volumetric and functional connectivity analyses.

Gray matter volume analysis

Voxel-Based Morphometry (VBM) analysis permits identification of regional gray matter volumetric decreases linked to processes like neuronal reorganization, reduced number of synapses, necrosis, and loss of cell density,[38] and volumetric increases related to augmented

synaptogenesis, neural hyper-activation, or the input of a constant stimulus.[39] This method has shown volumetric increases and decreases in other PNS diseases with axonal damage[19,20] and central inflammatory processes.[21–25]

We used the Diffeomorphic Anatomical Registration with the Exponentiated Lie algebra (VBM-DARTEL) algorithm,[40] within the Statistical Parametric Mapping toolbox (SPM8) in MATLAB, and the Statistical non-Parametric Mapping tool (SnPM) for statistical analysis (ref: https://warwick.ac.uk/snpm). The MPRAGE files were manually reoriented to the anterior commissure. DARTEL tools were used to segment different tissues types, creating probabilistic maps for each type. We then averaged all segmented images of each group and, after 6 iterations, created a group template by co-registering all the images in each group, followed by normalization to the Montreal Neurological Institute (MNI) stereotactic space. To this end we multiplied the produced image by the predetermined voxel volume of each area, therefore obtaining modulated images, which allow comparisons preserving the amount of brain tissue (e.g., volume). Finally, we smoothed all the images with an 8 mm full width half maximum Gaussian filter. The VBM whole-brain analysis consisted of one-sided two-sample t-tests between patients (PX) and controls (CT) (PX > CT and CT > PX). We used permutation tests using SnPM, establishing the null distribution in 10000 permutations. Only voxels with significant amount of gray matter in our final probabilistic maps were included (absolute voxel threshold of 0.2), preventing misclassification of low variance voxels and edge effects at tissue boundaries. We also used an additional explicit gray matter mask that was created through averaging of subjects' images. ANCOVA correction covariates comprised total intracranial volume (the sum of gray matter, white matter, and CSF volumes) and age. Clusters larger than 50 voxels (50 mm^3) passing voxel-level corrected significance threshold (familywise error (FWE) corrected to $P < 0.025$) are reported.

rsFC

To identify distributed changes to large-scale functional connectivity, it is useful to analyze the brain's intrinsic functional organization as a connected graph (the so-called human connectome), with brain regions represented as graph nodes, and connections between regions as graph edges.[41] Networks of changed connectivity in whole-brain graphs, for example, in patient-control comparisons, can be delineated using Network-Based Statistics (NBS) without a priori restriction to regions or networks of interest.[42] This method has been shown to elucidate the topological reorganization of brain pathologies such as mild cognitive impairment[43] and epilepsy.[44]

For rsFC analysis, fMRI volumes were slice-timing corrected and realigned for head motion correction using SPM12 within MATLAB. T1 Images were used to divide the brain into 160 anatomical regions (Destrieux atlas[45] + Freesurfer subcortical segmentation,[46] Freesurfer 5.3.0, https://surfer.nmr.mgh.harvard.edu/) in individual subject space. We chose this particular parcellation scheme in order to make results easily comparable to previous connectomics studies, and to allow automated objective extraction of clinically relevant anatomical labels. Atlas regions were coregistered to fMRI images using FSL (V5.0, https://fsl.fmrib.ox.ac.uk/). For each region, the temporal BOLD-signal averaged across all respective voxels was extracted. Six linear head motion parameters, CSF, white matter signal and global gray matter signals were regressed out of the averaged regional BOLD-signal. We used the R-Brainwaver package (V1.6, https://cran.r-project.org/web/packages/brainwaver/index.html) for wavelet transformation of the time series. We kept the third scale of the wavelet coefficients (according to a frequency of 0.031–0.63 Hz[47]). Pearson's correlation between those wavelet-filtered time series of each pair of the 160 extracted regions was calculated to define a whole-brain functional connectivity matrix. The correlation values were then Fisher z-transformed, resulting in a final 160 × 160 functional connectivity matrix. To identify networks of altered functional connectivity, the weighted and undirected connectivity matrices underwent statistical comparisons across patients and controls using NBS.[42] NBS is a nonparametric cluster-based approach to finding connected sets of nodes that significantly differ across connectivity matrices, controlled for multiple comparisons by comparing the found network size of significant nodes at an uncorrected statistical threshold to network sizes found when permuting group labels (here we use $n = 5000$ permutations). We report results at NBS-corrected threshold $P < 0.05$ following an auxiliary connection-wise threshold of $P < 0.0012$.

Results

Here, we employ VBM to localize potential volumetric gray matter changes, and NBS analysis of rsFC to investigate whether CNS manifestations in ZIKV patients may be linked to changes in the intrinsic functional network organization of the brain.

Gray matter volume

Using whole-brain analysis of gray matter (Fig. 1, Table 2), we found regional volumetric increase in right middle frontal gyrus in patients compared to controls. Contrastingly, we observed more widespread gray matter

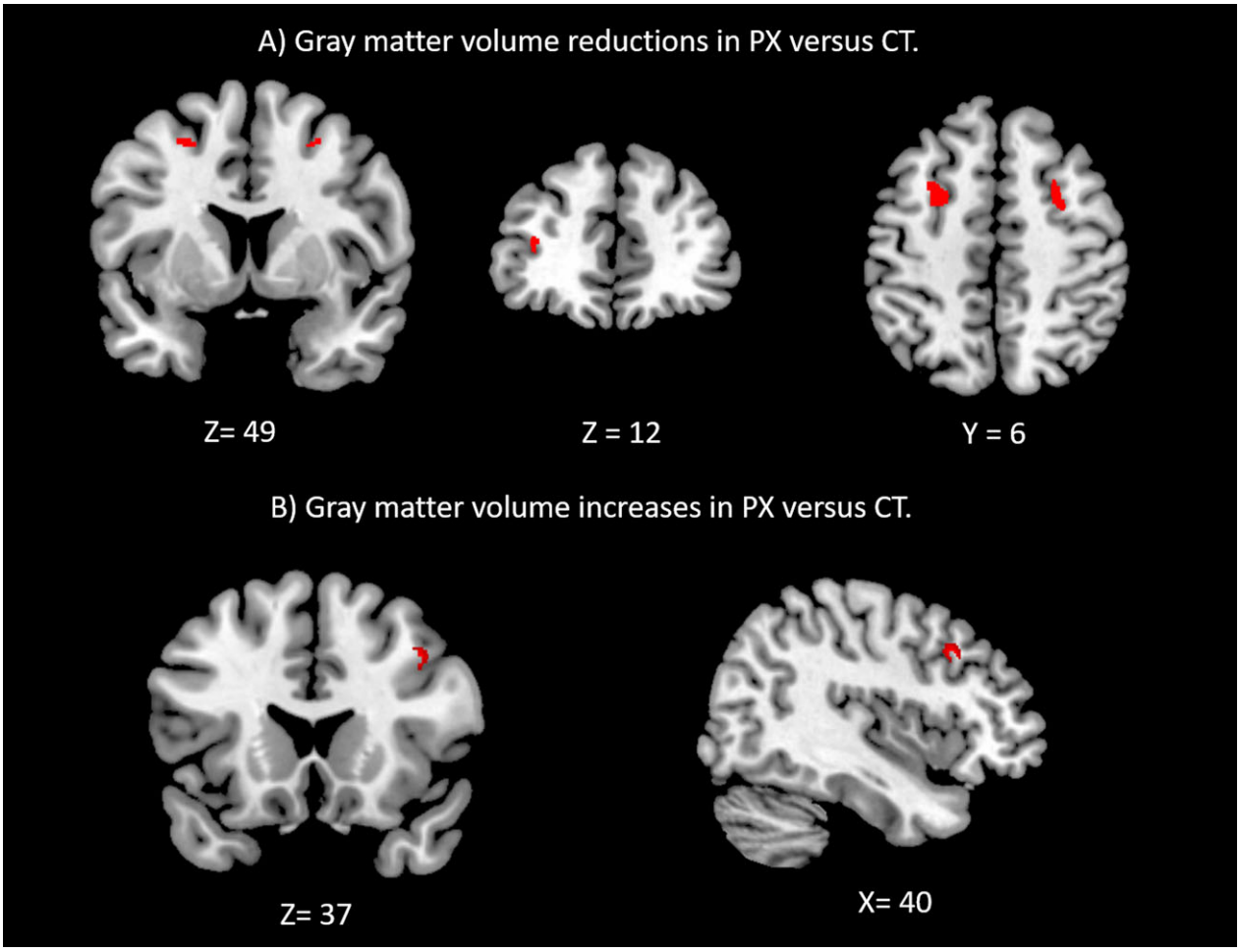

Figure 1. Gray matter volume decreases (A) and increases (B) in the ZIKV patient group compared to healthy controls (voxel-wise $P < 0.05$ FWE-corrected, cluster extent > 50 voxels (50 mm^3).

volume declines in bilateral supplementary motor area (SMA, specifically Frontal Eye Fields), and left inferior frontal sulcus.

rsFC

To better understand distributed changes in functional connectivity and alterations in complex topological network properties, we applied graph analysis and Network-Based Statistics to resting-state fMRI data. We observed a large-scale network of increased functional connectivity in ZIKV patients (*t*-test, single connection threshold $T \geq 3.6$, $P < 0.05$, NBS-corrected for multiple comparisons). This network was anchored in the temporal regions of the right hemisphere (centered in the superior temporal lobe and lateral sulcus) but also comprising interhemispheric connections to left temporal regions (Fig. 2). Detailed names and coordinates of the connected regions can be found in Table 3. No decreases in functional connectivity were observed.

Discussion

In this study, we report brain structural and functional changes in nine adults with previous ZIKV infection with central nervous system manifestations compared to age- and sex-matched healthy controls. The absence of other major neurological or systemic conditions unrelated to the ZIKV complications between infection and scan time, and persistence of particular ZIKV-related neurological symptoms at time of MRI scan (Table 1) speak to a link between the neuroimaging observations and the ZIKV-related neurological complications. We applied whole-brain analysis of volumetric differences in gray matter, and network-level analysis of rsFC. In the following, we will discuss our major findings: (1) the atypical

Table 2. VBM local maxima. Regions with significant gray matter volumetric changes for the VBM whole-brain analysis, Family-wise error (FWE) corrected at $P < 0.025$, extent > 50 voxels.

Volume increases (Patients > Controls)						
			MNI coordinates			
Peak voxel *p*	Cluster size	Peak voxel pseudo-*t*	*x*	*y*	*z*	Label
0.0003	100	7.70	40	21	37	R, Middle frontal gyrus
Volume decreases (Controls > Patients)						
			MNI coordinates			
Peak voxel *p*	Cluster size	Peak voxel pseudo-*t*	*x*	*y*	*z*	Label
0.0001	170	10.29	−26	7	49	L, Supplementary Motor Area (FEF)
0.0003	113	5.60	27	5	49	R, Supplementary Motor Area (FEF)
0.0006	61	7.61	−34	42	12	L, Inferior Frontal Sulcus

Labels: R, right hemisphere; L, left hemisphere; FEF, Frontal Eye Fields.

Guillain-Barre syndrome presentation associated with ZIKV infection in adults, (2) gray matter volumetric changes in the comparison of PX versus CT, and (3) increased bilateral temporal intra- and interhemispheric functional connectivity in PX > CT. While future studies are required to identify potential mechanisms underlying

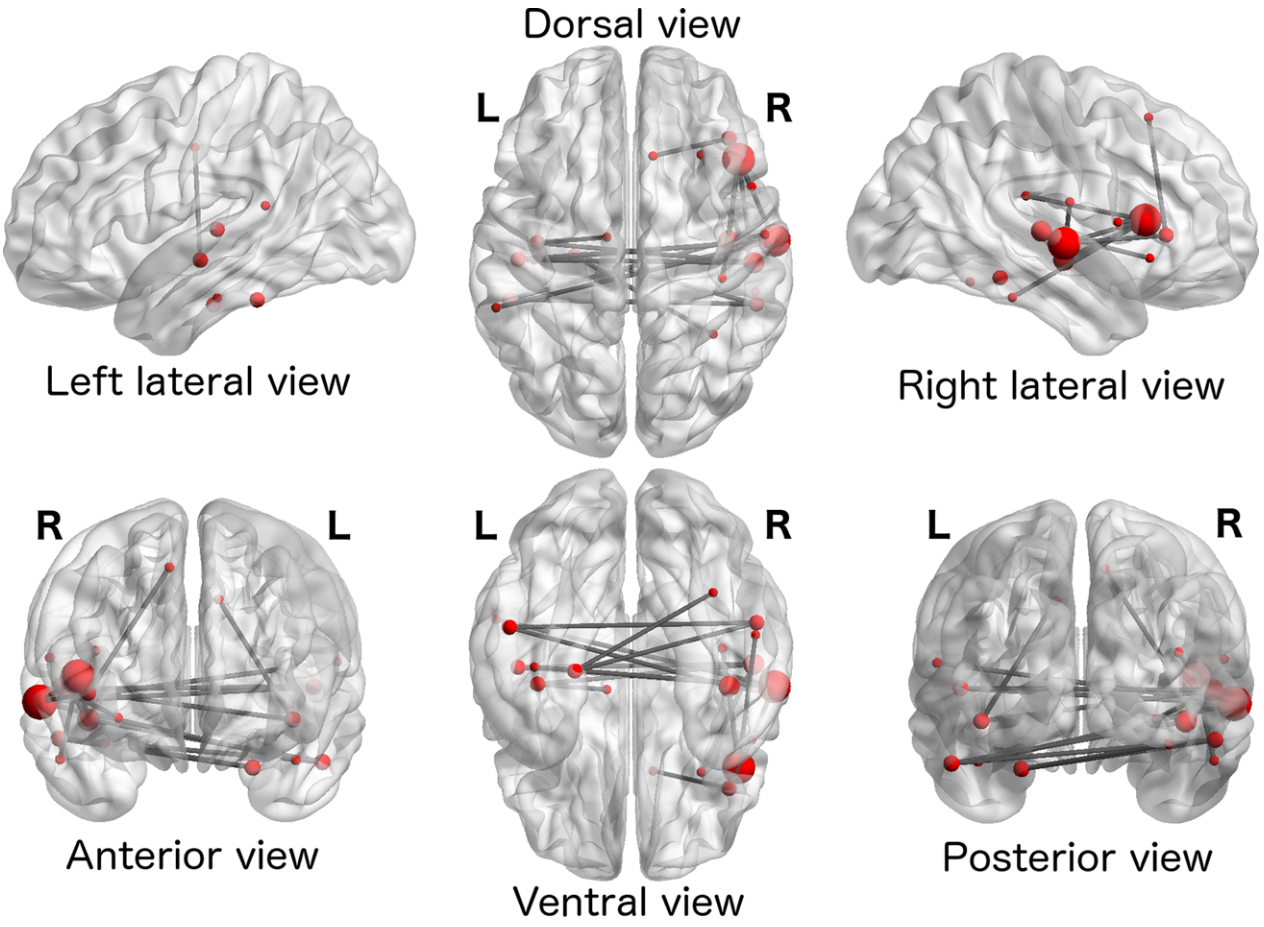

Figure 2. A large-scale network comprising nodes in right and left temporal cortices and right insula showed increased functional connectivity in ZIKV patients compared to healthy controls ($P < 0.05$ NBS-corrected for multiple comparisons, after an auxiliary single connection threshold of $T \geq 3.6$).

Table 3. Implicated regions in the network of increased connectivity in ZIKV patients (*t*-test Patient > Controls, single connection threshold $T \geq 3.6$, $P < 0.05$, NBS-corrected, l = left hemisphere, r = right hemisphere).

Hemi-sphere	Region	MNI coordinates	Number of connections
l	Midcingulate gyrus/sulcus - posterior part (pMCC)	−10 −12 40	1
l	Parahippocampal gyrus	−24 −19 −27	2
l	Heschl's gyrus	−48 −21 5	2
l	Superior temporal gyrus - planum temporale	−57 −41 15	1
l	Inferior temporal gyrus	−51 −38 −25	2
l	Insula - Inferior segment of the circular sulcus	−40 −14 −8	2
l	Transverse collateral sulcus - anterior part	−41 −21 −24	1
r	Subcentral gyrus/sulcus (central operculum)	57 −10 17	1
r	Inferior frontal gyrus - opercular part	51 10 8	1
r	Superior frontal gyrus	9 23 52	1
r	Fusiform gyrus	35 −53 −17	1
r	**Superior temporal gyrus - lateral aspect**	**61 −13 −1**	**5**
r	Inferior temporal gyrus	53 −35 −24	1
r	Lateral sulcus - horizontal ramus of the anterior segment	41 30 3	2
r	**Lateral sulcus - vertical ramus of the anterior segment**	**45 21 9**	**5**
r	Lateral sulcus - posterior segment	39 −29 19	1
r	Insula - anterior segment of the circular sulcus	30 23 −7	1
r	Insula - inferior segment of the circular sulcus	41 −13 −8	3
r	Inferior temporal sulcus	53 −40 −15	2
r	Transverse temporal sulcus	52 −22 4	3

Region labels are provided by the Destrieux atlas. Nodes with particularly large numbers of connections within the significant cluster are highlighted in bold face.

these alterations and to characterize differences in how Zika-related GBS and GBS of other etiologies might impact the brain structure and function, we cautiously offer potential interpretations of our findings in the following discussion. Each finding will be discussed in the context of the following alternatives that might explain the observed results: (1) Primary CNS impact of ZIKV, either due to direct viral invasion of the CNS, or inflammation ensuing from systemic ZIKV infection, (2) Secondary changes related to peripheral deafferentation, or (3) Secondary changes related to cognitive alterations caused by the illness.

Atypical Guillain-Barre syndrome and CNS symptoms in adults with ZIKV

Our patients had an atypical presentation of GBS, and further experienced CNS-related symptoms (Table 1). Typical GBS includes an ascending pattern of acute progressive limb weakness and areflexia explained by exclusive PNS damage.[48] Interestingly, six patients presented facial diplegia (rare GBS variant[49]) and descending weakness. This observation adds to reports of ZIKV-related GBS cases that follow a nontypical descending pattern.[10] Remarkably, the onset of the neurological symptoms occurred shortly after the Zika infection (Mean = 8.8days); contrastingly, GBS symptoms usually occur from 2 to 4 weeks following an antecedent infection.[48] This is in line with the report of parainfectious rather than the typical postinfectious GBS onset in about 50% of investigated ZIKV patients.[6,9] In addition, the motor symptoms were abruptly disabling, extending prior reports of a rapid progression.[6] This observation contrasts typical GBS: gradually manifested motor impairment, moving from ascending mild sensory loss within several days to weeks.[33] Furthermore, our EMG/NVC findings are suggestive of predominantly axonal damage, which deviates from typical GBS.[50]

Variations in GBS are usually associated with nonclassical pathophysiological features (e.g., type of nerve fibers affected, type of injury), commonly explained by the presence of antibodies to myelin glycolipids which are indicative of humoral autoimmunity.[49,51] Therefore, the above-described indications of atypical GBS presentations alongside CNS-symptoms in our patients may reflect an atypical pathophysiological mechanism (e.g., potential exaggerated/aggressive immunological response). In summary, our observations demonstrate the potential of ZIKV to cause a GBS variant and lead to CNS symptoms in adults, motivating future investigations into the pathophysiological mechanisms (autoimmune response involving specific anti-myelin antibodies). Because of the lack of a control group of GBS patients with non-Zika etiology, the following neuroimaging discussions are to be interpreted in the context of a polyradiculopathy versus healthy controls.

Gray matter volumetric changes

The CNS symptoms in our patients call for an investigation of how such symptoms manifest in the brain. Furthermore, to the best of our knowledge, no study has investigated the impact of PNS symptoms from GBS of any etiology on brain gray matter volume. In this study, we demonstrated gray matter alterations in a polyradiculopathy. In general, gray matter volume reductions likely reflect neuronal reorganization, reduced number of synapses, necrosis, or loss of cell density.[38] Consistent with the motor impairments, our patients, compared to healthy controls, exhibited reductions in gray matter in cortical regions involved in motor processing (bilateral SMA). These findings support the idea that prolonged decrease in peripheral motor action and somato-motor neural input negatively impacts gray matter volume. Notably, the SMA volume reductions correspond to left and right FEFs, key cortical nodes of the oculomotor system and, furthermore, core components of the Dorsal Attention Network underlying spatial attention.[52] An alternative interpretation could be that a temporary inflammatory injury of the FEFs may underlie diplopia observed in 6 of our patients, and may further exasperate perceptual deficits (e.g., dysmorphopsia and prosopagnosia) due to the role of this region in guiding visuo-spatial attention.

Importantly, regions beyond motor areas were also altered. These alterations comprised both volume decreases as well as increases in our subacute patients. Short-term volumetric increases may occur early in neuro-inflammation,[25] whereas long-term increases may reflect augmented synaptogenesis, the input of a constant stimulus, or neural hyperactivation.[38,39] We found gray matter volume reduction in right inferior frontal sulcus. From a network perspective, the particular location found to be reduced in this study is part of the Cingulo-Opercular network, which is implicated in maintaining tonic alertness.[53] Conversely, patients showed increases in gray matter volume in the right middle frontal gyrus. Interestingly, the middle frontal gyrus particularly in the right hemisphere has been proposed as the convergence center across the Dorsal Attention and Ventral Attention networks (see review by 54). Furthermore, several clinical studies have demonstrated that alterations in the right middle frontal gyrus (including the specific locus observed in this investigation) are linked to deficits in reorienting attention and spatial neglect.[55,56] Notably, all the observed nonmotor areas seem to play a key role in higher cognitive control, including top-down modulation of visual attention. Thus, their volumetric changes may be associated with the reported perceptual deficits.

Increased distributed functional connectivity in PX > CT

We observed a network of functional connectivity increases that were primarily centered on the right temporal lobe, and further extended to interhemispheric connections between the right and left temporal lobes. The distinctive anatomical and physiological features of the temporal lobes, such as presence of limbic and allocortical structures, make them particularly vulnerable to certain infectious, inflammatory and neurodegenerative diseases (see review 57). For instance, HSE predilection for the temporal lobe has been extensively documented,[58] and there are many other causes of Temporal Lobe Encephalitis associated with several infectious or noninfectious (e.g., autoimmune) etiologies.[59] Our functional connectivity observations thus support the hypothesis that ZIKV leads to an impact on CNS function, at least during the subacute phase.

A very broad range of neurological disorders are known to show a common pattern of large-scale functional connectivity changes: compensatory or dedifferentiation processes linked to increased functional connectivity at disease onset, followed by slowly decreasing connectivity in the subacute phase, and normalizing connectivity in the recovery phase.[28] This pattern is in line with our observed widespread connectivity increases in ZIKV during the subacute phase not yet having recovered to normal connectivity levels. Furthermore, increased functional connectivity has been linked to a fallback to structural connectivity in epilepsy patients,[44] anesthetized monkeys and at sleep onset.[60] Therefore, widespread increase in connectivity might point to reduced flexibility of brain function, and a limited functional repertoire.[61] In our patients, this suggested loss of functional flexibility is supported by the various perceptual abnormalities observed. This interpretation is especially compelling in light of the role of temporal cortices in uni- and multi-modal sensory processing and perceptual awareness.

Limitations

The rare subset of patients with CNS manifestations makes up a small proportion of adults with ZIKV infection, leading to a weakness of the current study in terms of the small number of patients. Despite this small number however, using different techniques (VBM and rsFC) we provide preliminary functional and structural evidence of consistent impact on the brain in a homogenous patient group.

Furthermore, this study is the first case–control neuroimaging study not only in adults with ZIKV, but also in patients with GBS-like presentation of any other

etiology. As such, we are providing the first data point that, due to its novelty, does not permit important comparisons with other patient groups. The ideal control population for our patients would consist of GBS cases of non-ZIKV etiology; however, GBS due to other causes is too infrequent to make recruitment feasible. While we may not claim that the observed results are exclusively related to *atypical* GBS, that is, dissociating contributions from GBS in general versus atypical manifestations specifically, we can draw conclusions about brain alterations linked to the full clinical profile.

Another consideration is that data were acquired in the subacute phase (5 ± 0.5 months since onset of neurological symptoms), such that normalization as well as compensatory mechanisms may have taken place between the acute infection and the MRI scans. Future comparisons with data from ZIKV patients of comparable clinical profile in the acute phase (i.e., within 2 weeks of onset) will support a dissociation between direct impact on the CNS (acute phase), versus late effects secondary to PNS weakness. Furthermore, future studies should consider follow up scanning (e.g., at one year post-onset) in order to determine whether our findings persist in the recovery phase of the GBS.

Conclusions

Taken together, our clinical observations comprised atypical descending and rapidly progressing PNS manifestations, and additional CNS neurological deficits. These observations strengthen prior evidence that ZIKV can cause a variant that deviates from the typical GBS profile. Whether GBS should be considered a variant in all or rather a subset of ZIKV patients with GBS-like symptoms is an open question. This question has momentous implications, for example, for choice of medication, where current recommendations for treatment of ZIKV-related neurological complications correspond to those for traditional GBS (immunoglobulin and plasmapheresis).

The deviation of neurological complications of ZIKV from typical PNS-only manifestations urgently calls for a characterization of potential impact on the CNS. In this first case–control neuroimaging study in adult ZIKV patients, we report impact on the brain both in gray matter volume as well as intrinsic functional organization. While some gray matter reduction occurred in motor-related regions likely secondary to prolonged PNS weakness, nonsomatomotor regions were also altered, indicative of PNS-independent effects. Intrinsic functional architecture measured by resting-state functional neuroimaging revealed increased functional connectivity in patients in line with compensatory or dedifferentiation processes. The connectivity changes were centered within and across temporal cortices, structures particularly vulnerable in a range of neurological conditions, and possibly linked to perceptual deficits.

To summarize, in studying a subset of severely affected adult ZIKV patients, our observations of CNS neurological deficits, volumetric changes especially outside of somato-motor areas, and changes of the intrinsic functional architecture centered on temporal lobes and insulae, demonstrate that the systemic infection can impact the brain. This highlights the urgent need for future studies into the underlying mechanisms to dissociate a possible direct viral infection of the CNS from an immune-mediated systemic response.

Acknowledgments

We thank Dr. Daniel A. Llano for constructive feedback on the manuscript.

Author Contributions

Conception and Design of the Study: R.B.M., J.W., P.S., S.S. Acquisition and Analysis of Data: R.B.M., J.W., M.R., L.T., P.S., J.O., I.M., P.B., S.S. Manuscript and Figures Preparation: R.B.M., J.W., I.M., S.S.

Conflicts of Interest

Nothing to report.

References

1. Blázquez A-B, Saiz J-C. Neurological manifestations of Zika virus infection. World J Virol 2016;5:135.
2. WHO. 2017. WHO|Zika situation report. Available from: http://www.who.int/emergencies/zika-virus/situation-report/10-march-2017/en/ (Last accessed: 7 September 2017)
3. Dick GWA. 1952. Zika virus (II). Pathogenicity and physical properties. Trans R Soc Trop Med Hyg 46:521–534.
4. Rasmussen SA, Jamieson DJ, Honein MA, Petersen LR. Zika virus and birth defects—reviewing the evidence for causality. N Engl J Med 2016;374:1981–1987.
5. van de Beek D, Brouwer MC. CNS Infections in 2016: 2016, the year of Zika virus. Nat Rev Neurol 2017;13:69–70. advance online publication. Available from: http://www.nature.com/nrneurol/journal/vaop/ncurrent/full/nrneurol.2016.202.html?WT.feed_name=subjects_genetics (last accessed: 30 January 2017).
6. Cao-Lormeau V-M, Blake A, Mons S, et al. Guillain-Barré Syndrome outbreak associated with Zika virus infection in French Polynesia: a case-control study. Lancet 2016;387:1531–1539.
7. Frontera JA, da Silva IR. Zika getting on your nerves? The association with the Guillain–Barré syndrome. Mass

Medical Soc 2016;375:1581–1582. Available from: http://www.nejm.org/doi/full/10.1056/NEJMe1611840 (last accessed: 8 February 2017).
8. Machado-Alba JE, Machado-Duque ME, Gaviria-Mendoza A, Orozco-Giraldo V. Diagnosis of neurological disorders and the Zika virus epidemic in Colombia 2014–2016. Int J Infect Dis 2016;51:133–134.
9. Parra B, Lizarazo J, Jiménez-Arango JA, et al. Guillain-Barré Syndrome associated with Zika virus infection in Colombia. N Engl J Med 2016;375:1513–1523.
10. Kassavetis P, Joseph J-MB, Francois R, et al. Zika virus–associated Guillain-Barré syndrome variant in Haiti. Neurology 2016;87:336–337.
11. Muñoz LS, Barreras P, Pardo CA. Zika virus-associated neurological disease in the adult: guillain-barré syndrome, encephalitis, and myelitis. Semin Reprod Med 2016;34:273–279.
12. WHO/PAHO. 2017. Zika - Epidemiological Update. Available from: http://www.paho.org/hq/index.php?option=com_docman&task=doc_view&Itemid=270&gid=40945&lang=en (last accessed: 7 September 2017)
13. Barcellos C, Xavier DR, Pavão AL, et al. Increased hospitalizations for neuropathies as indicators of zika virus infection, according to health information system data. Brazil. Emerg. Infect. Dis. 2016;22:1894–1899.
14. Galliez RM, Spitz M, Rafful PP, et al. Zika virus causing encephalomyelitis associated with immunoactivation. Open Forum Infect Dis 2016;3:4. Available from: https://academic.oup.com/ofid/article/3/4/ofw203/2445907/Zika-Virus-Causing-Encephalomyelitis-Associated (last accessed: 30 January 2017).
15. Mécharles S, Herrmann C, Poullain P, et al. Acute myelitis due to Zika virus infection. Lancet 2016;387:1481.
16. Soares CN, Brasil P, Carrera RM, et al. Fatal encephalitis associated with Zika virus infection in an adult. J Clin Virol 2016;83:63–65.
17. Brito-Ferreira ML. Zika virus may now be tied to another brain disease. Am Acad Neurol 2016;95:1405–1409. Available from: https://www.ajtmh.org/content/journals/10.4269/ajtmh.17-0106. https://doi.org/10.4269/ajtmh.17-0106
18. Carteaux G, Maquart M, Bedet A, et al. Zika virus associated with meningoencephalitis. N Engl J Med 2016;374:1595–1596.
19. Selvarajah D, Wilkinson ID, Maxwell M, et al. Magnetic resonance neuroimaging study of brain structural differences in diabetic peripheral neuropathy. Diabetes Care 2014;37:1681–1688.
20. Lu Y, Liu H, Hua X, et al. Attenuation of brain grey matter volume in brachial plexus injury patients. Neurol Sci 2016;37:51–56.
21. Gitelman DR, Ashburner J, Friston KJ, et al. Voxel-based morphometry of herpes simplex encephalitis. NeuroImage 2001;13:623–631.
22. Frisch S, Thiel F, Marschhauser A, et al. Identifying neural correlates of memory and language disturbances in herpes simplex encephalitis: a voxel-based morphometry (VBM) study. J Neurol 2015;262:563–569.
23. Küper M, Rabe K, Esser S, et al. Structural gray and white matter changes in patients with HIV. J Neurol 2011;258:1066–1075.
24. Puri BK, Jakeman PM, Agour M, et al. Regional grey and white matter volumetric changes in myalgic encephalomyelitis (chronic fatigue syndrome): a voxel-based morphometry 3 T MRI study. Br J Radiol 2012;85:e270–e273.
25. Wagner J, Weber B, Elger CE. Early and chronic gray matter volume changes in limbic encephalitis revealed by voxel-based morphometry. Epilepsia 2015;56:754–761.
26. He BJ, Shulman GL, Snyder AZ, Corbetta M. The role of impaired neuronal communication in neurological disorders. Curr Opin Neurol 2007;20:655–660.
27. Zhou J, Gennatas ED, Kramer JH, et al. Predicting regional neurodegeneration from the healthy brain functional connectome. Neuron 2012;73:1216–1227.
28. Fornito A, Zalesky A, Breakspear M. The connectomics of brain disorders. Nat Rev Neurosci 2015;16:159–172.
29. Finke C, Kopp UA, Scheel M, et al. Functional and structural brain changes in anti-N-methyl-D-aspartate receptor encephalitis: Finke et al.: MRI in Anti-NMDAR Encephalitis. Ann Neurol 2013;74:284–296.
30. Ann HW, Jun S, Shin N-Y, et al. Characteristics of resting-state functional connectivity in HIV-associated neurocognitive disorder. PLoS ONE 2016;11:e0153493.
31. Brier MR, Day GS, Snyder AZ, et al. N-methyl-D-aspartate receptor encephalitis mediates loss of intrinsic activity measured by functional MRI. J Neurol 2016;263:1083–1091.
32. Ropper AH, Wijdicks EFM, Truax BT. Guillain- Barre syndrome. Philadelphia: Oxford University Press, 1991.
33. Dimachkie MM, Barohn RJ. Guillain-Barré syndrome and variants. Neurol Clin 2013;31:491–510.
34. Gordon PH, Wilbourn AJ. Early electrodiagnostic findings in Guillain-Barré syndrome. Arch Neurol 2001;58:913–917.
35. Power JD, Barnes KA, Snyder AZ, et al. Spurious but systematic correlations in functional connectivity MRI networks arise from subject motion. NeuroImage 2012;59:2142–2154.
36. Dickie DA, Mikhael S, Job DE, et al. Permutation and parametric tests for effect sizes in voxel-based morphometry of grey matter volume in brain structural MRI. Magn Reson Imaging 2015;33:1299–1305.
37. Winkler AM, Ridgway GR, Webster MA, et al. Permutation inference for the general linear model. NeuroImage 2014;92:381–397.
38. Anderson BJ. Plasticity of gray matter volume: the cellular and synaptic plasticity that underlies volumetric change. Dev Psychobiol 2011;53:456–465.
39. Teutsch S, Herken W, Bingel U, et al. Changes in brain gray matter due to repetitive painful stimulation. NeuroImage 2008;42:845–849.

40. Ashburner J. A fast diffeomorphic image registration algorithm. NeuroImage 2007;38:95–113.
41. Bullmore E, Sporns O. Complex brain networks: graph theoretical analysis of structural and functional systems. Nat Rev Neurosci 2009;10:186–198.
42. Zalesky A, Fornito A, Bullmore ET. Network-based statistic: identifying differences in brain networks. NeuroImage 2010;53:1197–1207.
43. Wang J, Zuo X, Dai Z, et al. Disrupted functional brain connectome in individuals at risk for Alzheimer's Disease. Biol Psychiatry 2013;73:472–481.
44. Wirsich J, Perry A, Ridley B, et al. Whole-brain analytic measures of network communication reveal increased structure-function correlation in right temporal lobe epilepsy. Neuroimage Clin 2016;11:707–718.
45. Destrieux C, Fischl B, Dale A, Halgren E. Automatic parcellation of human cortical gyri and sulci using standard anatomical nomenclature. NeuroImage 2010;53:1–15.
46. Fischl B, Salat DH, Busa E, et al. Whole brain segmentation. Neuron 2002;33:341–355.
47. Achard S, Salvador R, Whitcher B, et al. A resilient, low-frequency, small-world human brain functional network with highly connected association cortical hubs. J Neurosci 2006;26:63–72.
48. van Doorn PA, Ruts L, Jacobs BC. Clinical features, pathogenesis, and treatment of Guillain-Barré syndrome. Lancet Neurol. 2008;7:939–950.
49. Susuki K, Koga M, Hirata K, et al. A Guillain-Barré syndrome variant with prominent facial diplegia. J Neurol 2009;256:1899–1905.
50. Jacobs BC, Meulstee J, van Doorn PA, van der Meché FGA. Electrodiagnostic findings related to anti-GM1 and anti-GQ1b antibodies in Guillain-Barré syndrome. Muscle Nerve 1997;20:446–452.
51. Hafer-Macko CE, Sheikh KA, Li CY, et al. Immune attack on the schwann cell surface in acute inflammatory demyelinating polyneuropathy. Ann Neurol 1996;39: 625–635.
52. Corbetta M. Frontoparietal cortical networks for directing attention and the eye to visual locations: identical, independent, or overlapping neural systems? Proc Natl Acad Sci USA 1998;95:831–838.
53. Sadaghiani S, D'Esposito M. Functional characterization of the cingulo-opercular network in the maintenance of tonic alertness. Cereb Cortex 2015;25:2763–2773.
54. Corbetta M, Patel G, Shulman GL. The reorienting system of the human brain: from environment to theory of mind. Neuron 2008;58:306–324.
55. Japee S, Holiday K, Satyshur MD, et al. A role of right middle frontal gyrus in reorienting of attention: a case study. Front Syst Neurosci 2015;9:23.Available from: https://www.ncbi.nlm.nih.gov/pmc/articles/PMC4347607/ (last accessed: 23 February 2018)
56. He BJ, Snyder AZ, Vincent JL, et al. Breakdown of functional connectivity in frontoparietal networks underlies behavioral deficits in spatial neglect. Neuron 2007;53:905–918.
57. Eran A, Hodes A, Izbudak I. Bilateral temporal lobe disease: looking beyond herpes encephalitis. Insights Imaging 2016;7:265–274.
58. Demaerel P, Wilms G, Robberecht W, et al. MRI of herpes simplex encephalitis. Neuroradiology 1992;34:490–493.
59. Sureka J, Jakkani RK. Clinico-radiological spectrum of bilateral temporal lobe hyperintensity: a retrospective review. Br J Radiol 2012;85:e782–e792.
60. Tagliazucchi E, Laufs H. Decoding wakefulness levels from typical fMRI resting-state data reveals reliable drifts between wakefulness and sleep. Neuron 2014;82: 695–708.
61. Barttfeld P, Uhrig L, Sitt JD, et al. Signature of consciousness in the dynamics of resting-state brain activity. Proc Natl Acad Sci 2015;112:887–892.

